ISSN 2176-5480

22nd International Congress of Mechanical Engineering (COBEM 2013)
November 3-7, 2013, Ribeirão Preto, SP, Brazil

EXPERIMENTAL INVESTIGATION OF POWER HARVESTING IN A MECHANICALLY EXCITED PIEZOELECTRIC BEAM

Wescley Oliveira Viana Barbosa
Aline Souza de Paula
Universidade de Brasília - Department of Mechanical Engineering
70.910.900 - Asa Norte – Brasília – DF - Brazil
wescleycris@gmail.com, alinedepaula@unb.br

Abstract. *The search for renewable energy sources is increasingly growing in recent decades. In this context, several studies explore the use of piezoelectric materials in the energy harvesting from mechanical energy, present in the ambient, into electrical energy. When subjected to external mechanical loads, piezoelectric materials produce a distribution of electric charges on their surfaces (direct piezoelectric effect). Moreover, when subjected to external electric fields, these materials exhibit variations on its shape and dimensions (inverse piezoelectric effect). For energy harvesting purpose the direct effect is explored. Basically the piezoelectric material is attached to a vibrant structure and while the structure vibrates, the material is deformed, generating electricity. This paper addresses an experimental investigation of the energy harvesting performance of a piezoelectric MFC beam. The goal of the study is to evaluate the influence, in power conversion, when different electrical circuits are attached to the MFC beam. The device is subjected to harmonic base excitation in a frequency range that encompasses the first resonance frequency. In all analyzed cases, the provided mechanical power, the generated electrical power and the efficiency in the conversion are evaluated. The analysis is carried out experimentally.*

Keywords: *Piezoelectric beam, MFC, power harvester, experimental.*

1. INTRODUCTION

Piezoelectric materials are intelligent materials that exhibit coupling between two physical domains: mechanical and electrical. Due to this electromechanical coupling it is possible to convert mechanical into electrical energy or vice versa (Leo, 2007). In the first case, external mechanical loads produce a distribution of electrical charges on their surfaces, known as piezoelectric direct effect. By exploring this effect, traditionally piezoelectric materials are used as sensors (Galhardi et al., 2008). Moreover, when subjected to external electric fields, these materials exhibit changes in their shape and dimensions, known as inverse piezoelectric effect. In this case, the material operates as the actuator and can be used, for example, in vibration control (Flatau and Chong, 2002).

The energy problem has been exhaustively discussed in recent decades due to the increase in energy consumption, and issues related to fossil fuel reduction and environmental preservation. This concern has motivated many researchers to develop techniques for obtaining renewable energy sources (Poizot & Dolhem, 2011; Gkoumas *et al.*, 2012), such as solar, wind, fluid flow, gravity and thermal gradients (Panwara *et al.*, 2011). In addition to these sources, the energy present in the mechanical vibrations, that are available in the environment, has been attracting attention.

In this context, researches attention concerning piezoelectric materials has turned to the use of these materials for converting mechanical energy into electrical energy. These devices, known as energy harvesters or power harvesters (Anton & Sodano, 2007), can be used to charge electrical circuits that require low power supply, such as wireless monitoring sensors and microelectromechanical systems, MEMS (Hehn *et al.*, 2009; Jeon *et al.*, 2005; Galhardi *et al.*, 2008; Liu *et al.*, 2008; Renno *et al.*, 2009; Vuller *et al.*, 2009).

Traditionally, these energy harvesters consist of piezoelectric elements attached to a beam with one free end and the other end fixed to a vibration source. As a consequence of the mechanical vibration, the material is deformed, generating electricity due to the direct piezoelectric effect. Several authors assume simplified model for this system, by considering a mass-spring-damper system operating at resonance (Ferrari *et al.*, 2009; Triplett and Quinn, 2009; Cottone *et al.*, 2012 Minazara *et al.*, 2008; Ye *et al.* 2009). Numerous studies report the use of piezoelectric materials for power harvesting purposes (Sodano *et al.*, 2004; Ricart *et al.*, 2010; Kanno *et al.*, 2010; Erturk, 2011; Gkoumas *et al.*, 2012; Andosca *et al.*, 2012; Minazara *et al.*, 2008). In order to improve the power generation and increase the efficiency of Power Harvesting systems, several studies have incorporated electrical circuits to these devices (Szarka *et al.*, 2012, Do *et al.*, 2011, Rocha *et al.*, 2010; Howells 2009; Saggini *et al.*, 2010; Turner *et al.*, 2012; Ammar & Basrour, 2006; Marinkovic *et al.*, 2009; Hehn *et al.*, 2009; Lefeuvre *et al.*, 2006).

This paper addresses an experimental investigation of the power harvesting performance of a harmonically excited MFC piezoelectric beam attached to an electrical circuit. The considered device is similar to the ones used by Sodano & Inman (2004), Triplett & Quinn (2009), Ricart *et al.* (2010) and Kanno *et al.* (2010). The goal of the study is to evaluate the influence on the power harvesting when different electrical circuits (R, RC, RL and RLC), with different resistive and reactive loads, are attached to the MFC beam. The device is subjected to harmonic base excitation in a frequency range that encompasses the first resonance frequency. In all analyzed cases, the provided mechanical power, the

ISSN 2176-5480

generated electrical power and the efficiency in the conversion are evaluated. Results are discussed with the purpose of defining a more suitable circuit for future applications involving energy storage.

It is important to mention that in this study resistive and reactive loads are inserted in series with the MFC piezoelectric beam. This configuration is different from those considered in previously cited works. When subjected to harmonically mechanical excitation, the beam generates an AC voltage due to the electromechanical coupling. This voltage can be influenced by inductive and capacitive reactance. The presence of capacitive reactance advance electric current when compared to the voltage. The use of an inductor or a capacitor, however, can reduce this lag between voltage and current, increasing system efficiency. Ammar & Basrour (2006), Hehn *et al.* (2009), Kwon & Ricon-Mora (2009), Saginni *et al.* (2010) and Turner *et al.* (2012) shows how the use of inducers influences the performance of piezoelectric power harvesting devices. Different from the present work, however, these authors use drives synchronized and controlled by transistors.

2. PIEZOELECTRIC POWER HARVESTING DEVICE

Similar to Sodano & Inman (2004), Triplett & Quinn (2009), Ricart *et al.* (2010), Kanno *et al.* (2010) the system considered in this work consists of a MFC piezoelectric beam free in one end and subjected to a harmonic base excitation at the other end. In the present work, the analysis is carried out experimentally. However, in this section, it is presented a simplified model of the piezoelectric power harvesting device and a brief theory, in order to improve the understanding of the analysis evaluated experimentally. After that, the experimental setup is presented.

2.1 Model and theory

Figure 1 presents a schematic picture of the MFC piezoelectric beam (a) and equivalent model commonly used for the power harvesting device (b).

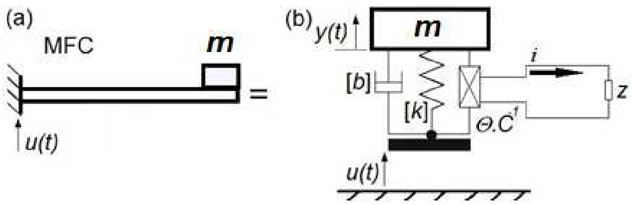

Figure 1. Piezoelectric power harvesting device. (a) MFC piezoelectric beam, (b) Equivalent mass-spring-damper system coupled to a circuit (similar to Priya & Inman, 2008; Triplett & Quinn, 2009).

The mechanical part is commonly model as a 1 DOF mass-spring-damper, as shown in Figure 1(b). The electrical part and the coupled circuit, also indicated in figure 1(b), are used to evaluate the generated electrical power. The variable m represents the concentrated mass, k is the elastic stiffness, b represents the linear viscous damping, Θ is the electromechanical coupling coefficient of piezoelectric material, C is the piezoelectric capacitance and i is the electric current in the circuit. The charge Z is the impedance of the coupled circuit. In this work, the electric circuit consists of resistive loads, which can be capacitive and/or inductive. Furthermore, the coordinate u(t) is the base displacement, while y(t) is the relative displacement of the mass.

By considering a harmonic base excitation $u(\mathrm{t})=A\sin(\omega \mathrm{t})$, the equation of motion of the system is given by Eq. (1).

$$m\ddot{y} + b\dot{y} + ky - \Theta(y)QC^{-1} = mA\omega^2 \sin(\omega \mathrm{t}). \qquad (1)$$

where Q is the electrical charge in the circuit coupled to the piezoelectric beam. The generated voltage in the piezoelectric element, in response to vibrations, is given by the following relation (Triplet and Quinn, 2009):

$$V = -\,\Theta(y)C^{-1}y + QC^{-1}. \qquad (2)$$

From the first Ohm's Law:

$$V = Zi. \qquad (3)$$

where the impedance, Z , represents the total load of the circuit.

The electrical power generated by piezoelectric beam when coupled to an electric circuit composed of resistors, inductors and capacitors, is calculated in terms of the voltage V, generated by the beam, the total electric current i which runs the electric circuit and the angle ϕ represents the phase angle between the voltage and the total current running through the circuit.

Thus, the electrical power generated is obtained from equation:

ISSN 2176-5480

$$P_G = V\, i\, cos\phi. \tag{4}$$

However, according to equations (3) and (4), the generated electric power can also be calculated by Eq. (5).

$$P_G = V^2 Z^{-1} cos\phi. \tag{5}$$

On the other hand, the supplied mechanical power can be calculated by Eq. (6).

$$P_S = F\, \dot{u}\, cos\, \Theta \tag{6}$$

where F is the force applied to the beam, $\dot{u}$ is the exciting base velocity and Θ is the phase angle between F and $\dot{u}$. Thus the efficiency of the power harvesting is given by Eq. (7).

$$\eta = \frac{P_G}{P_S} \times 100 \quad (\%) \tag{7}$$

In the present work, the analysis is carried out experimentally. However, the mathematical model and a brief theory are presented to improve the understanding of the studied system.

2.2 Experimental setup

The MFC piezoelectric beam analyzed in this work is the model M2814-P2 from the *Smart Materials Corp*. The piezoelectric element dimensions are 28 x 14 mm and the capacitance is 25,7η*F*, the beam overall dimensions are 37 x 18 mm. The beam is fixed to an electrodynamic shaker (*Labworks Inc.* model ET127), which provides the harmonic excitation of the system, by a metallic support. The control of the shaker is provided by the controller *Data Physics Signalstar Scalar Abacus Lite*. A PCB Piezotronics accelerometer model 352C34, used as control accelerometer, is fixed on the base of the shaker and connected to one of the input channels of the controller. This sensor has a sensitivity of 100mV/g, works in the frequency range from 0.5 to 10 kHz with a measure range of ± 50 g peak and has a mass of 5.8g.

In addition to the control accelerometer (used exclusively to the control of the shaker), a second accelerometer, PCB Piezotronics 352C33, is used to measure the shaker acceleration. This sensor has the same characteristics of the PCB 352C34. A force sensor Piezotronics model 208C03, attached to the metallic support, is used to obtain the force. The 208C03 force sensor has a sensitivity of 10 mV/lb (2,248 mV / kN), 500 lbs (2,224 kN) static tension and compression, the maximum compression force of 3000 pounds (13.5 kN) and the maximum static tensile strength 500 lbs (2,224 kN), resolution bandwidth from 1 to 10 kHz (0.005 lb-rms / rms-0.02N) and the excitation voltage VDC 20 to 30. At last, the circuit coupled to the beam is mounted in a protoboard. Experimental setup details are shown in Figure 2.

(a) (b) (c)

Figure 2. Experimental setup details. a) Piezoelectric beam attached to metallic support, accelerometer and force sensor; b) Beam attached to the shaker and control accelerometer; c) Protoboard.

For data acquisition, monitoring and signal processing it is used a chassis with two modules and software *Labview*, all from National Instruments. The chassis is the cDAQ NI USB-9178, that has 8-slot, 15 W and input voltage range of 9-30 V. The modules NI 9201 and NI 9234 are connected to the chassis. The NI 9201 is a module with 8 analog input channels for measuring voltage and maximum sampling rate of 500 kS/s connectors with screw terminals and maximum voltage range of ±10 V. The NI 9234 is a module with 4 channels of high precision frequency measurement and sampling rate of 51,2 kS/s, BNC connectors, ideal for signal conditioning of sensors, such as accelerometers, load cells and microphones. The maximum voltage range is ± 5 V.

By integrating the acceleration of the base of the shaker, measured by NI 9234, and using the information of the measured force, *F*, it is possible to calculate the power supplied to the piezoelectric beam, by using Eq. (6). The

ISSN 2176-5480

electrical power is evaluated from the voltage, measured by NI 9201, and current in the circuit by using Eq. (4). Due to the unavailability to measure current directly, this quantity is obtained by means of a shunt resistor (80Ω).

Figure 3 shows the flow diagram of the procedure evaluated experimentally.

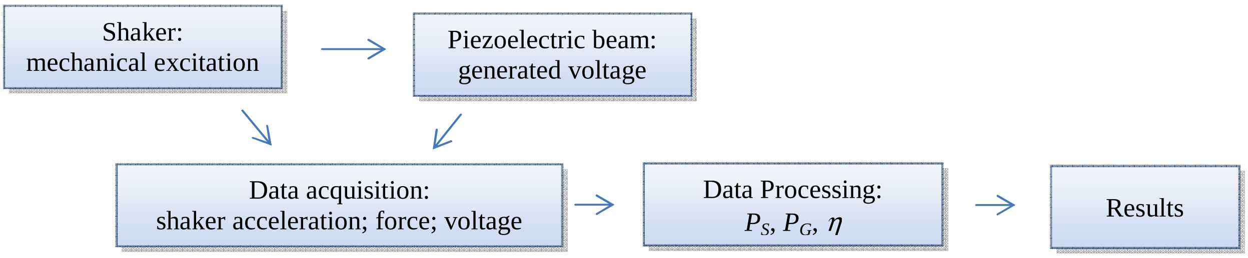

Figure 3. Flow diagram of experimental procedure.

3. RESULTS

Initially, it is interesting to identify the resonant frequency of the system, where highest amplitude oscillation of the beam is obtained. By evaluating a sweep, the first resonant frequency is identified near 17 Hz. Therefore, in all analysis that are carried out, it is considered a frequency range from 16.8Hz to 17.8 Hz. For each excitation frequency, system response is monitored during 25.0s after reaching steady state. Supplied mechanical power, generated electrical power and efficiency in the conversion are evaluated in all cases.

The results are divided in five subsections in other to evaluate the influence of: base oscillation amplitude; and different circuits: resistive (R), resistive-capacitive (RC), resistive-inductive (RL) and resistive-inductive-capacitive (RLC). Each circuit coupled to the MFC beam is associated in series with an 80 Ω resistor and introduced between terminals A and B, as presented in Figure 4. The 80 Ω resistor is used to obtain the electrical current.

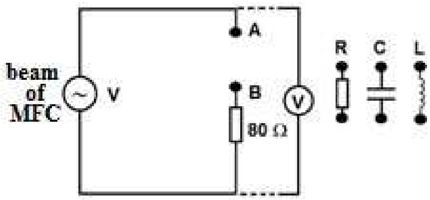

Figure 4. Electrical circuit used in the tests. R – resistor, C – capacitor, L – inductor.

3.1 Base oscillation amplitude variation

At first, base oscillation amplitude variation is of concern. Three amplitudes are evaluated: 0.5 mm, 0.75 mm and 1.0 mm peak to peak in the frequency range of 16.8 Hz to 17.8 Hz. Figure 5 shows supplied mechanical power, generated electrical power and efficiency. Table 1 shows the results related to the maximum electrical power obtained for each base amplitude. For higher base oscillations amplitude, higher electrical power is obtained. However, it can be observed that efficiency in the conversion is compatible in all amplitudes since supplied mechanical power also inceases for higher base excitations amplitudes.

Table 1. Results related to the maximum generated electrical power for different base oscillation amplitudes.

Amplitude (mm)	Resonance Frequency (Hz)	Voltage (V)	Mechanical Power (mW)	Electrical Power (mW)	Efficiency (%)
0.50	17.40	0.64	54.90	0.18	0.33
0.75	17.30	0.86	108.95	0.33	0.30
1.00	17.30	1.12	182.49	0.56	0.31

ISSN 2176-5480

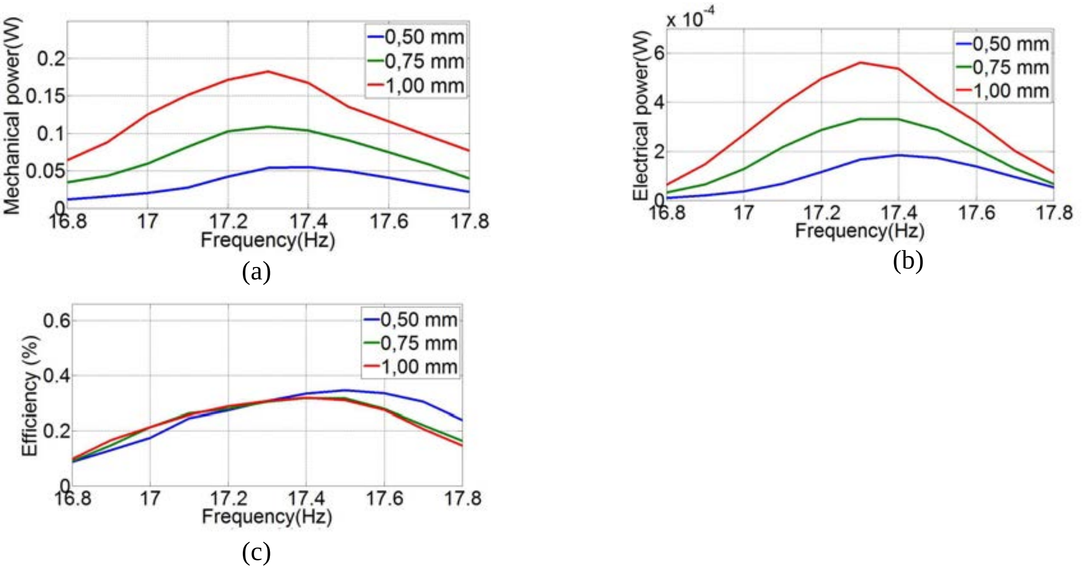

(a) (b) (c)

Figure 5. Results for different base oscillation amplitudes: a) Supplied mechanical power; b) Generated electrical power; c) Efficiency.

3.2 R Circiut

At this point, the influence of a coupled R circuit, inserted between terminal A and B as presented in Figure 4, is carried out. In this analysis, constant base oscillation amplitude of 1 mm is considered and three different resistors are evaluated: 2.14 kΩ, 4.56 kΩ and 8.14 kΩ. Figure 6 shows supplied mechanical power, generated electrical power and efficiency, while Table 2 shows the results related to the maximum electrical power obtained for each resistence.

The supplied mechanical power is equal in all three analyzed cases, as the base amplitude is constant, and is shown in Figure 6(a). From Figure 6(b) it is observed that electrical power increases when the resistance of the circuit is increased. This same tendency can be observed in the efficiency, Figure 6(c). A considerable percentage increase in the maximum efficiency can be observed for higher resistive couple circuit, as shown in Table 2. At this point, it is important to mention that for resistive loads, the voltage and electric current are in phase.

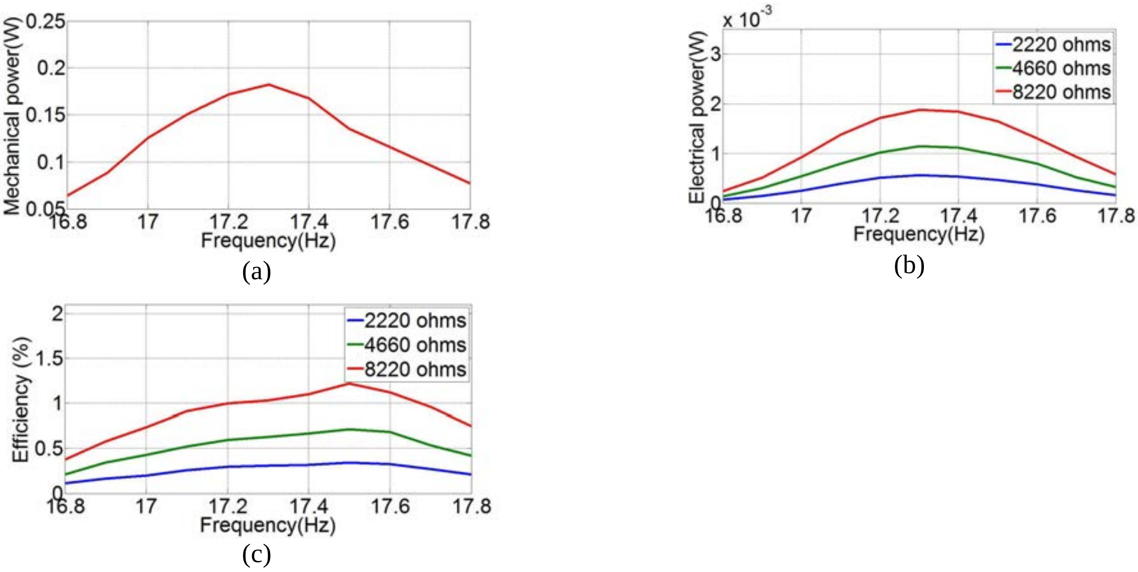

(a) (b) (c)

Figure 6. R circuit influence results: a) Supplied mechanical power; b) Generated electrical power; c) Efficiency.

Table 2. Results related to the maximum generated electrical power for R circuit.

Amplitude (mm)	Resonance frequency (Hz)	Equivalent resistance (kΩ)	Voltage (V)	Mechanical Power (mW)	Electrical Power (mW)	Efficiency (%)
1.00	17.30	2.22	1.12	182.49	0.56	0.31
1.00	17.30	4.66	2.31	182.49	1.33	0.63
1.00	17.30	8.22	3.90	182.49	1.90	1.03

3.3 RC Circuit

Now, the influence of a coupled RC circuit, inserted between terminal A and B as presented in Figure 4, is carried out. As in R circuit analysis, constant base oscillation amplitude of 1 mm is considered. Three electrolytic capacitors are considered with capacitances: 1.0 µF, 2.2 µF and 4.7 µF. Moreover, an 80 Ω resistance is considered, as shown in Figure 4. It is important to mention that the capacitors were chosen so that the values of the capacitive reactance are equivalent to those used in the resistive circuit considered in previous analysis.

Figure 7 shows generated electrical power and efficiency, while Table 3 shows the results related to the maximum electrical power obtained for each capacitor. Supplied mechanical power is equal to the result obtained for R circuit analysis (Figure 6(a)) since the same base amplitude excitation is considered. From the presented results it can be observed that electrical power increases when the capacitance of the circuit is higher. This same tendency can be observed in the efficiency of the system. The percentage of the increase in the efficiency, however, is smaller when compared to the resistive circuit. Moreover, it can be observed that the efficiency obtained in RC circuit is considerably smaller than in R circuit, even with equivalent capacitive reactance. This fact is explained by the phase angle between voltage and current that occurs due to the presence of the capacitor.

It is important to mention that the inclusion of a capacitor in series with the piezoelectric beam, which also has a capacitance, produces a decrease in the system equivalent capacitance. This reduction in capacitance increases the voltage generated by the beam once the capacitance is inversely proportional to the voltage between the plates of a capacitor.

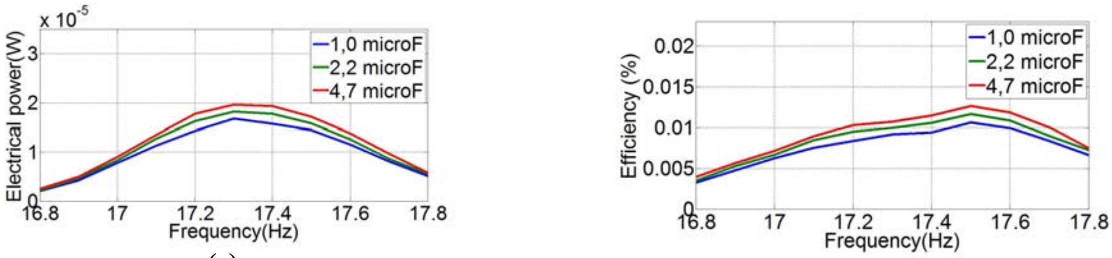

Figure 7. RC circuit influence results: a) Generated electrical power; b) Efficiency.

Table 3. Results related to the maximum generated electrical power for RC circuit.

Amplitude (mm)	Resonance frequency (Hz)	Capacitance (µF)	Voltage (V)	Mechanical Power (mW)	Electrical Power (µW)	Efficiency (%)
1.00	17.30	1.0	4.21	182.49	16.7	0.009
1.00	17.30	2.2	1.99	182.49	18.2	0.010
1.00	17.30	4.7	0.97	182.49	19.6	0.011

3.4 RL Circuit

The third circuit analyzed is the RL circuit, which is inserted between terminal A and B as presented in Figure 4. As in R and RC circuit analysis, constant base oscillation amplitude of 1 mm is considered. Due to the difficulty of finding inductors with high inductances commercially, three inductors are built in the laboratory, with the winding of 2200 turns, 4220 turns and 8000 turns of fine enameled copper wire on a PVC pipe 40 mm x 10 mm. The inductors built present approximately 150 mH, 346 mH and 611 mH. The reactance estimated in resonance frequency is 16.30Ω, 37.71Ω and 66Ω, respectively. These values are below the order of magnitude of the loads tested previously in R and RC circuits. The inductance necessary should be, at least, 80 H. Thus, it was not possible to consider inductive reactance equivalent to previous analyzed cases.

ISSN 2176-5480

Figure 8 shows generated electrical power and efficiency, while Table 4 shows the results related to the maximum electrical power obtained for each capacitor. Supplied mechanical power is again equal to the result obtained for R circuit analysis (Figure 6(a)) since the same base amplitude excitation is considered.

From the presented results it can be noticed that electrical power increases when the inductance of the circuit is higher. This same tendency can be observed in the efficiency of the system. The voltage obtained with the inductors is much lower than the evaluated voltage with resistors and capacitors. However, it is important to highlight that the magnitude order of inductive reactance is $10^1\Omega$, while for R and RC circuit the magnitude order is $10^3\Omega$. Besides the generated voltage is smaller, the electrical power is considerably higher than the results obtained RC circuit. This is an interesting result that can be explained due to a small phase angle between voltage and current when compared to resistive-capacitive case. When compared to purely resistive circuit, the generated electrical power is smaller.

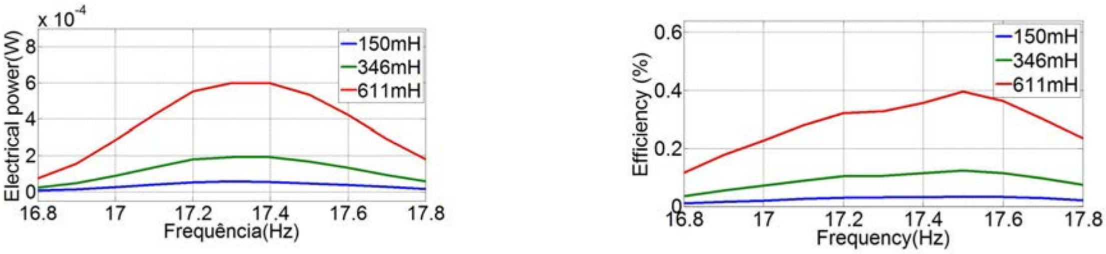

(a) (b)

Figure 8. RL circuit influence results: a) Generated electrical power; b) Efficiency.

Table 4. Results related to the maximum generated electrical power for RL circuit.

Amplitude (mm)	Resonance frequency (Hz)	Indutance (mH)	Voltage (V)	Mechanical Power (mW)	Electrical Power (mW)	Efficiency (%)
1.00	17.30	150	0.09	182.49	0.06	0.03
1.00	17.30	346	0.15	182.49	0.20	0.11
1.00	17.30	611	0.24	182.49	0.60	0.33

3.5 Circuit RLC and comparison.

Finally, it is evaluated a comparative analysis of the beam when coupled to all different analyzed circuits: resistive (R); resistive - capacitive (RC); resistive - inductive (RL) and resistive - inductive - capacitive (RLC). It is important to highlight that, in these tests, the impedances have the same magnitude order. Table 5 shows loads values coupled to the beam and connected to terminals AB of Figure 4.

Table 5. Different circuits loads.

Circuits	Resistance (Ω)	Capacitance (μF)	Inductance (mH)
R	80	0	0
RC	80	68	0
RL	80	0	346
RLC-A	80	68	150
RLC-B	80	68	346

Figure 9 shows generated electrical power and efficiency, while Table 6 shows the results related to the maximum electrical power obtained for each circuit. Supplied mechanical power is again equal to the result obtained for R circuit analysis (Figure 6(a)) since the same base amplitude excitation is considered.

ISSN 2176-5480

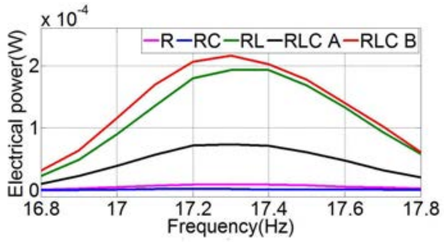

(a)

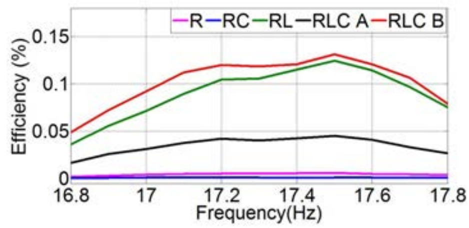

(b)

Figure 8. Comparison between R, RC, RL and RLC circuits results: a) Generated electrical power; b) Efficiency.

Besides the generated voltage, electrical power and efficiency evaluated in previous cases, phase angle between voltage and electric current, $\emptyset$, is also evaluated and presented in Table 6. It is important to highlight that the MFC piezoelectric beam used in this study has a capacitance of approximately 25.8 ηF and an electrical resistance around 108 Ω. Although these parameters varies according to the deformation of the beam, it is reasonable considering that phase angle produced by the electrical impedance of the beam is very small. Thus, the phase differences observed in the tests are due to resistive and reactive loads inserted in the electrical circuit.

Table 6. Results related to the maximum generated electrical power for R, RL, RC, RLC A and RLC B circuits.

Amplitude (mm)	Resonance Frequency (Hz)	Voltage (V)	Mechanical Power (mW)	Electrical Power (mW)	Efficiency (%)	Phase Angle V x i (°)
R	17.3	0.04	182.49	0.001	0.005	0.772
RC	17.3	0.08	182.49	0.002	0.001	-88.3
RL	17.3	0.15	182.49	0.193	0.110	4.12
RLC-A	17.3	0.11	182.49	0.074	0.040	-52.3
RLC-B	17.3	0.16	182.49	0.216	0.118	-30.5

Concerning the phase angle, we can conclude that purely resistive circuit has no influence and phase angle is near to zero. When a capacitor or inductor is added to the circuit, a phase angle between voltage and current appears. However, it is interesting to note that, although the voltage and current are in phase in the circuit purely resistive, the voltage and electric power are lower when compared to the results obtained for RL circuit. This fact can be explained once the inductor is a device capable of storing energy in the form of magnetic field. This device opposes the change in magnetic field and consequently the variation in electric current. This reaction is responsible for obtaining higher electrical voltage in the system. Capacitors also store energy by accumulating electric charge between their plates. This energy is stored in the form of an electric field.

The piezoelectric beam harmonically excited consists in an alternating current source that provides an electrical voltage to the circuit that constantly changes its polarity. This causes the electric current of the circuit to reverse its sense. In turn, the magnetic field of the inductor, which has stored energy, changes its direction. This change in the magnetic field of the inductor causes it to discharge the stored energy in the circuit. As the circuit receives power from piezoelectric beam and reactive power inductor, discharged during the current direction reversal, there is an increase in the energy of the system. This behavior also occurs in the RLC circuit. However, the inductor and capacitor exchange energy among themselves during the changes in electric current sense. This exchange of energy between the capacitor and inductor, added to the constant voltage supply from the piezoelectric beam, increases energy of the system.

The cited interaction between capacitor and inductor also influences phase angle between the voltage and current, which is fundamental to electrical power generation. Note that RLC-A presents a phase angle smaller that RC circuit. By considering an inductor with a higher inductance, in RLC-B circuit, the absolute phase angle is even smaller, increasing the generated electrical power and, consequently, the efficiency. Even though circuits RL and RLC-B have the same inductance of 346 mH and phase angle of the RL circuit is smaller, the RLC-B circuit is more efficient due to the energy exchange between the inductor and capacitor. The use of higher inductances in RLC circuit will decrease even more the phase angle between voltage and current and, consequently, increase system efficiency.

4. CONCLUSION

This paper presents an analysis, carried out experimentally, of the energy harvesting performance of a MFC piezoelectric beam harmonically excited when coupled to different electric circuits and operating near the first resonance frequency. Four circuits are analyzed: resistive (R), resistive-capacitive (RC), resistive-inductive (RL) and resistive-inductive-capacitive (RLC), and the performances are evaluated by means of generated electrical power and efficiency.

Before evaluating different circuits, the influence of base excitation amplitude is investigated. It is observed that the increase of the base amplitude causes an increase in generated electrical power. However, there is no increase in the efficiency, which presents a similar behavior and values for all different base amplitude considered, once the increase of the amplitude excitation also causes an increase of the supplied mechanical power.

In the analysis of R, RC and RL circuits it is observed that an increase of the resistance, capacitance and inductance, respectively, produces an increase in the generated electrical power and, consequently, in the efficiency. An important influence of phase angle between voltage and current is observed in the system efficiency.

By comparing R and RC circuits, with equivalent reactance, the resistive circuit presents a better performance, once the resistive circuit does not causes a phase angle and resistive-capacitive circuit presents a considerable lag between voltage and current. By considering RL circuit, also with equivalent reactance, the performance of the power harvesting system is better than using R circuit even with the lag between voltage and current caused by the presence of the inductor.

By considering the RLC-A circuit, the absolute phase angle is smaller than in RC circuit and the efficiency is greater than R and RC circuits, but smaller than RL. By increasing the inductivity, RLC-B circuit, a smaller absolute phase angle than the one obtained with RLC-A is observed and the efficiency increases, reaching the better performance from the analyzed circuits. This increase in the generated electrical power observed in the RLC circuit can be explained by the energy exchange that occur between the capacitor and inductor and also due to a decrease in absolute phase angle.

It is important to highlight that the goal of the present work was not to obtain the maximum possible efficiency of the system, but to compare the influence of different circuits, by considering components with compatible reactance, in the electrical energy generation. The efficiency of the energy harvester, however, can be increased with appropriate dimensioning of resistive and reactive loads and appropriate circuit coupled to the beam. The use of these piezoelectric generators may be interesting in the supply of low-power devices.

5. ACKNOWLEDGEMENTS

The authors would like to acknowledge the support of the Brazilian Research Agency CNPq and through the INCT-EIE (National Institute of Science and Technology – Smart Structures in Engineering) the CNPq and FAPEMIG.

6. REFERENCES

Ammar, Y.; Basrour, S. Non-linear Techniques for Increasing Harvesting Energy from Piezoelectric and Electromagnetic Micro-Power Generators. Design, Test, Integration and Packaging of MEMS/MOEMS DTIP. Stresa, Lago Maggiore, Italy: [s.n.]. 2006.

Andosca, R; MCDonald, T. Gus; Genova, V; Rosenberg, Steven; Keatingd, Joseph; Benedixen, Cole; Wu, Junru. Experimental and theoretical studies on MEMS piezoelectric vibrational energy harvesters with mass loading. Sensors and Actuators A: Physical, v. 178, p. 76-87, mAY 2012.

Anton, S. R.; Sodano, H. A. A review of power harversting using piezoelectrics materials (2003-2006). Smart Materials and Structures, v. 16, n. 3, p. 1-21, May 2007.

Cottone, F; Gammaitoni, L.; Vocca, H.; Ferrari, M.; Ferrari, V. Piezoelectric buckled beams for random vibration energy harvesting. Smart Materials and Structures, v. 21, p. 1-12, Febraury 2012. ISSN 3.

Do, Xuan-Dien; Ko, Young-Hun; Nguyeb, Huy-Hieu; Le, Huy-Binh; Lee, Sang-Gug. An efficient parallel SSHI rectifier for piezoelectric energy scavenging systems. 13th International Conference on Advanced Communication Technology (ICACT). Phoenix Park, Korea (South): IEEXplore. 2011. p. 1394-1397.

Erturk, A. Piezoelectric energy harvesting for civil infrastructure system applications: Moving loads and surface strain fluctuations. Journal of Intelligent Material Systems and Structures, v. 22, n. 17, p. 1959-1973, November 2011.

Ferrari, M.; Ferrari, V; Guizzetti, Michele; Andô, Bruno; Baglio, Salvatori; Trigona, Carlo. Improved Energy Harvesting from Wideband Vibrations by Nonlinear Piezoelectric Converters. Procedia Chemistry, v. 1, n. 1, p. 1203-1206, september 2009.

Flatau, A. B.; Chong, K. P. Dynamic smart material and structural systems. Engineering Structures, Volume 24, v. 24, n. 3, p. 261-270(10), March 2002.

Galhardi, M. A.; Guilherme, T. H.; Júnior, V. L. A Review of Power Harvesting on Mechanical Vibration. 7th Brazilian Conference on Dinamics, COntrol and Aplications. Presidente Prudente, São Paulo: [s.n.]. 2008. p. 1-9

Gkoumas, K.; Gaudenzi, O. D; Petrini, F. Energy Harvesting applications in transportation infrastructure networks. Procedia – Social and Behavioral Sciences, v. 48, n. issue especial Transport Research Arena 2012, p. 1097–1107., 2012.

Hehn, T.; Hargerdon, F.; Manoli, Y. Highly Efficient Energy Extraction from Piezoelectric Generators. Procedia Chemistry, v. 1, n. 1, p. 1451-1454, September 2009.

Howells, C. A. Piezoelectric energy harvesting. Energy Conversion and Management, v. 50, n. 7, p. 1847-1850, July 2009.

Jeon, Y. B; Sood, R.; Jeong, J.-H.; Kim, S.-G. MEMS power generator with transverse mode thin film PZT. Sensors and Actuators A: Physical, v. 122, n. 1, p. 16-22, july 2005.

Kanno, I; Sagawa, K.; oka, R.; Kotera, H.; Ogawa, J.; Yanauchi, N.; Aizawa, K.; Matsushima, T. Piezoelectric Energy Harvesters of PZT films deposited on Titanium Cantilervers. Proceedings Power MEMS. Leuven, Belgium: [s.n.]. 2010. p. 379-382.

Kwon, D.; Rincon-mora, G. A. A Rectifier-Free Piezoelectric Energy Harvesting Circuit. IEEE International Symposium on Digital Object Identifier, p. 1085-1088, May 2009.

Lefeuvre, E; Badel, A; Richard, C; Guyomar, D; Pettit, L. Petit. Optimization of piezoelectric electrical generators powered by random vibrations. Symposium Design, Test, Integration and Packaging of MEMS/MOEMS. Stresa, Lago Maggiore, Italy: [s.n.]. 2006.

Leo, D. J. Engineering Analysis of Smart Material Systems. Hobokeb, New Jersey: John wiley & Sons, 2007.

Liu, J.-Q; Fang, Hua-Bin; Xu, Zheng; Mao, Xix-Hui; Shen, N, Xiu-Cheng; Chen, Di; Liao, Huang; Cai, Bing-Chu. A MEMS based piezoelectric power generator array for vibration energy harvesting. Microelectronics Journal , v. 39, n. 5, p. 802-806, may 2008.

Marinkovic, D; Frey, Alexader; Kuehne, Ingo; Scholl, Gerd. A New Rectifier and Trigger Circuit for a Piezoelectric Microgenerator. Procedia Chemistry, v. 1, n. 1, p. 1447-1450, September 2009.

Minazara, E.; Vasic, D.; Costa, F. Piezoelectric Generator Harvesting Bike Vibrations Energy to Supply Portable. International Conference on Renewable Energier and Power Quality. Santander: [s.n.]. 2008. p. 1-6.

Panwara, N.L; Kaushokb, S. C.; Kotharia, Surendra. Role of renewable energy sources in environmental protection: A review. Renewable and Sustainable Energy Reviews, v.15, n. 03, April 2011, p. 1513–1524.

Poizot, P.; Dolhem, F. Clean energy new deal for a sustainable world: from non-CO2 generating energy sources to greener electrochemical storage devices. Energy & Environmental Science, v. 4, n. 6, p. 2003-2019, 2011.

Renno, J. M.; Daqaq, M. F.; Inman, D. J. On the optimal energy harvesting from a vibration source. Journal of Sound and Vibration, v. 320, n. 1-2, p. 386-405, February 2009.

Ricart, T; Defay, E; Abergeli, J.; Rascle, A; Rhun, G.L.; LassagneASSAGNE, P.; perruchot, F; Aid, M. Cantilers with piezoelectric thin films for weakly vibrating environment. Proceedings Power MEMS. Leuven, Belgium: [s.n.]. 2010. p. 83-86.

Rocha, J. G.; Gonzálves, P.F.; Rocha, P. F.; Silva, M. P.; Lanceros, S. Energy Harvesting From Piezoelectric Materials Fully Integrated in Footwear. IEEE Transactions on Industrial Electronics, v. 57, n. 3, p. 813-819, March 2010.

Saggini, S; Giro, S.; Ongar, F.; Mattavelli, P. Implementation of Reactive and Resistive Load Matching for Optimal Energy Harvesting from Piezoelectric Generators. IEEE 12th Workshop on Control and Modeling for Power Electronics (COMPEL). Colorado, USA: [s.n.]. 2010. p. 1-6.

Shen, Dongna. Piezolectric Energy Harvesting Devices for Low Frequency Vibration Applications. 194p. Tese (Doutorado em Filosofia) - Auburn University, Alabama, 2009.

Sodano, H. A.; Inman, D. J. Estimation of Electric Charge Output for Piezoelectric Energy Harvesting. Strain Journal, v. 40, n. 2, p. 49-58, May 2004.

Turner, J; Ahmed, Maruf N.; Ha Dong Sam; Mattavelli, Paolo. A new approach to the wide bandwidth of piezoelectric transducers for vibration energy harvesting. IEEE 55th international Midwest Symposium. Boise, Idaho - USA: [s.n.]. 2012. p. 1064-1067.

Triplett, A.; Quinn, D. D. The Effect of Non-linear Piezoelectric Coupling on Vibration-based Energy Harvesting. Journal of Intelligent Material Systems and Structures, v. 20, p. 1959-1967, November 2009. ISSN 16.

Ye, G; Yan ,Jize; Wong, Zi Jing; Soga, KEnichi; Seshia, Ashwin. Optimisation of a Piezoelectric System for Energy. International Ultrasonics Symposium (IUS). Roma, Italy: IEEEXplore. 2009. p. 759-762.

7. RESPONSIBILITY NOTICE

The authors are the only responsible for the printed material included in this paper.